Numerical Methods in Civil Engineering, 10-2 (2025) 44-59

Numerical Methods in Civil Engineering

Journal Homepage: https://nmce.kntu.ac.ir/

Simulation of flow features in the face of tainter and sluice gate flow measurement structures

Hamidreza Abbaszadeh*, Kiyoumars Roushangar, Rasoul Daneshfaraz***, John Abraham******

ARTICLE INFO

RESEARCH PAPER

Article history:
Received:
December 2025
Revised:
December 2025
Accepted:
December 2025

Keywords:
Sluice-tainter gate
Suppressed and non-suppressed sill
Hydraulic performance
nonlinear relation
Numerical solution

Abstract:

Gates are structures that permit water flow underneath the gate. They are important water-management structures and require careful design by engineers. The aim of this research is to numerically evaluate the effect of a sill on the hydraulic flow characteristics through sluice and tainter gates using the volume of fluid (VOF) method. Sills with various geometric characteristics were simulated. The findings indicated that the RNG turbulence model had the highest accuracy compared to k-ε, k-ω, and LES. The discharge coefficient (C_d) with a sill is higher than without a sill. Among the investigated sills, the semicircular sill C_d is greater than that of the rectangular one. In addition, the C_d of the tainter gate exceeds that of the sluice for regardless of whether a sill is used. Increasing the thickness of the sill leads to increases in the shear stress of the flow, and consequently, the flow rate decreases. The C_d with a gate with a sill always exceeds the value without a sill. On the other hand, the C_d increases with the increase of the sill height up to a certain level and then decreases thereafter.

1. Introduction

Water management is becoming increasingly challenging due to changes in both water demand and availability. This issue is made more complex because of climate change which makes efficient water management increasingly important. Control of water flow and distribution in irrigation networks is important to prevent water wastage. To assist with water management, gates can be used as flow-control devices. Gates should be carefully designed and selected based on the specific needs of an application. Examining the hydraulic performance of gates is one of the most significant issues in engineering. The most widely used gates are sluice and tainter gates (vertical and cylindrical plates). When the gate height exceeds a specific design criterion, multiple gates are used [1].

In recent years, many studies have been conducted on gates. Henry [2] determined the discharge coefficient (C_d) of gates. Rajaratnam and Subramanya [3] Rajaratnam [4], and Swamee [5] investigated the C_d of sluice gates and presented relations for estimating *its* value. Shivapur and Prakash [6] explored the position of a sluice gate at various angles. The results indicated that C_d increases with increasing angle. Bijankhan et al. [7] presented analytical results to distinguish the condition curves of radial gates. In addition, they investigated the available calibration methods for the radial gates. Daneshfaraz et al. [8] studied the impact of gate edge shape on contraction coefficients through the use of a numerical model. Their findings revealed that gates with sharp and rounded edges experience a decrease in contraction coefficients when the G/E_0 (G=gate opening, E_0= specific energy) is less than 0.4, but an increase for ratios greater than 0.4. Shayan et al. [9] carried out a study on radial gate flow using E-M equations. They established equations grounded in theory that are suitable for predicting discharge from a radial gate under actual operating

* *Corresponding author: Department of Civil Engineering, Faculty of Civil Engineering, University of Tabriz, Tabriz, Iran. Email: ha.abbaszadeh@tabrizu.ac.ir*
** *Department of Civil Engineering, Faculty of Civil Engineering, University of Tabriz, Tabriz, Iran.*
*** *Department of Civil Engineering, Faculty of Engineering, University of Maragheh, Maragheh, Iran.*
**** *School of Engineering, University of St. Thomas, St. Paul, MN 33901, USA.*

https://doi.org/10.61882/NMCE.2512.1113

conditions. The proposed equations are efficient in estimating flow with a satisfactory level of accuracy. Salmasi et al. [10] investigated the C_d of inclined sluice gates using intelligent models. They reported that C_d increases as the gate angle increases. Roushangar et al. [11] checked the C_d of tainter gates using soft computing methods. Examination of various models showed that the Gaussian process regression performs better than the support vector machine.

Regarding a sill application with a sluice gate, we can refer to Alhamid's [12] experimental study. Their results indicated an increase in the C_d when a sill is employed. Abdelhaleem [13] conducted a study on radial gates and sills and found that the variation in contraction coefficient is primarily influenced by the height of the sill. Salmasi and Norouzi [14] studied how the shape of the sill affects the C_d of the sluice gate. Their findings indicated that the sill increases C_d by 23% to 31%. Salmasi et al. [15] evaluated the effect of the suppressed sill on the C_d of the radial gate. Their investigation showed that an upstream sill position acts as a barrier and reduces the C_d. Karami et al. [16] checked out the C_d of sluice gates with sills. Their findings revealed that the presence of a sill increases C_d. Ghorbani et al. [17] used soft computing models to analyze the C_d of sluice gates with a suppressed sill. Their findings indicated that the H_2O model effectively predicts C_d for sluice gates. Norouzi et al. [18] investigated the vortex upstream of the sluice gate with a sill. The findings revealed that the use of the sill reduces the amount of air entering the water. As the sill width increases, the water vortex decreases. Hassanzadeh and Abbaszadeh [19] investigated the C_d of a sluice gate with a sill using intelligent models. The results indicated that the ANN model outperformed the SVM and KNN models in predicting C_d. The results of Daneshfaraz et al. [20] indicated that the discharge coefficient increases by installing the sill at certain intervals at increasing distance with respect to the upstream of the sluice gate and has a lower value compared to the non-sill state. Daneshfaraz et al [21] investigated the C_d of the gate experimentally and numerically. Their findings indicated that the C_d with a sill in the tangent position upstream of the gate is higher than the downstream tangent and below situations.

The analysis of flow characteristics in tainter and sluice gate structures is crucial. Accurate simulation of these features can provide valuable insights into the behavior of water flow. It is possible to gain a better understanding of the hydraulic performance of these structures and make informed decisions about their design and operation. The research background indicates that most of the studies were conducted for sluice gate C_d values. A study on the use of a non-suppressed sill with various geometrical characteristics with a tainter gate has not been previously performed. This is an important subject for designers of water management structures, and the information provided in this study fills a knowledge gap in that area.

2. Materials and methods

2.1 Governing equations

The FLOW-3D software was used to discretize the geometry and solve the continuity and Navier-Stokes equations of fluid motion. The relation of continuity for flow is [22]:

$$\frac{\partial \rho}{\partial t} + \frac{\partial}{\partial x_i}(\rho u_i) = 0 \quad (1)$$

where u_i is the component of the velocity vector in the direction of i. The Navier Stokes equations are generally expressed as Equation 2 [22]:

$$\rho\left(\frac{\partial u_i}{\partial t} + u_j \frac{\partial u_i}{\partial x_i}\right) = -\frac{\partial P}{\partial x_i} + B_i + \frac{\partial}{\partial x_j}\left[\mu\left(\frac{\partial u_i}{\partial x_j} + \frac{\partial u_j}{\partial x_i} - \frac{2}{3}\delta_{ij}\frac{\partial u_k}{\partial x_k}\right)\right] \quad (2)$$

In Equation 2, B_i represents the volumetric force, μ is the dynamic viscosity, ρ is the specific gravity of water, $x_{(i,j,k)}$ is the flow coordinates, and δ_{ij} shows the Kronecker delta. For δ_{ij}, if $i=j$ it is equal to 1, and otherwise it is equal to zero.

2.2 Dimensional analysis

Validation was performed using the experimental data of Daneshfaraz et al. [20] for the sluice gate. Simulations were included for additional models including the sluice gate and the tainter gate with various sill shapes and different geometrical specifications (Table 1). Fig. 1 provides illustrations of the models.

Table 1: Model Characteristics

Gate type		Upstream depth (m)	Flow rate (m^3/s)
sluice-tainter (R=0.30 m)		0.05-0.42	0.0025-0.0142
Gate opening (m)	Height of sills (m)	Thickness of sills (m)	Width of sills (m)
0.01, 0.02 and 0.04	0.03, 0.06 and 0.09 (rectangular-semicircular)	0.05, 0.15- and 0.25 (rectangular) 0.06, 0.12 and 0.18 (semicircular)	0.15, 0.20 and 0.30 (rectangular-semicircular)

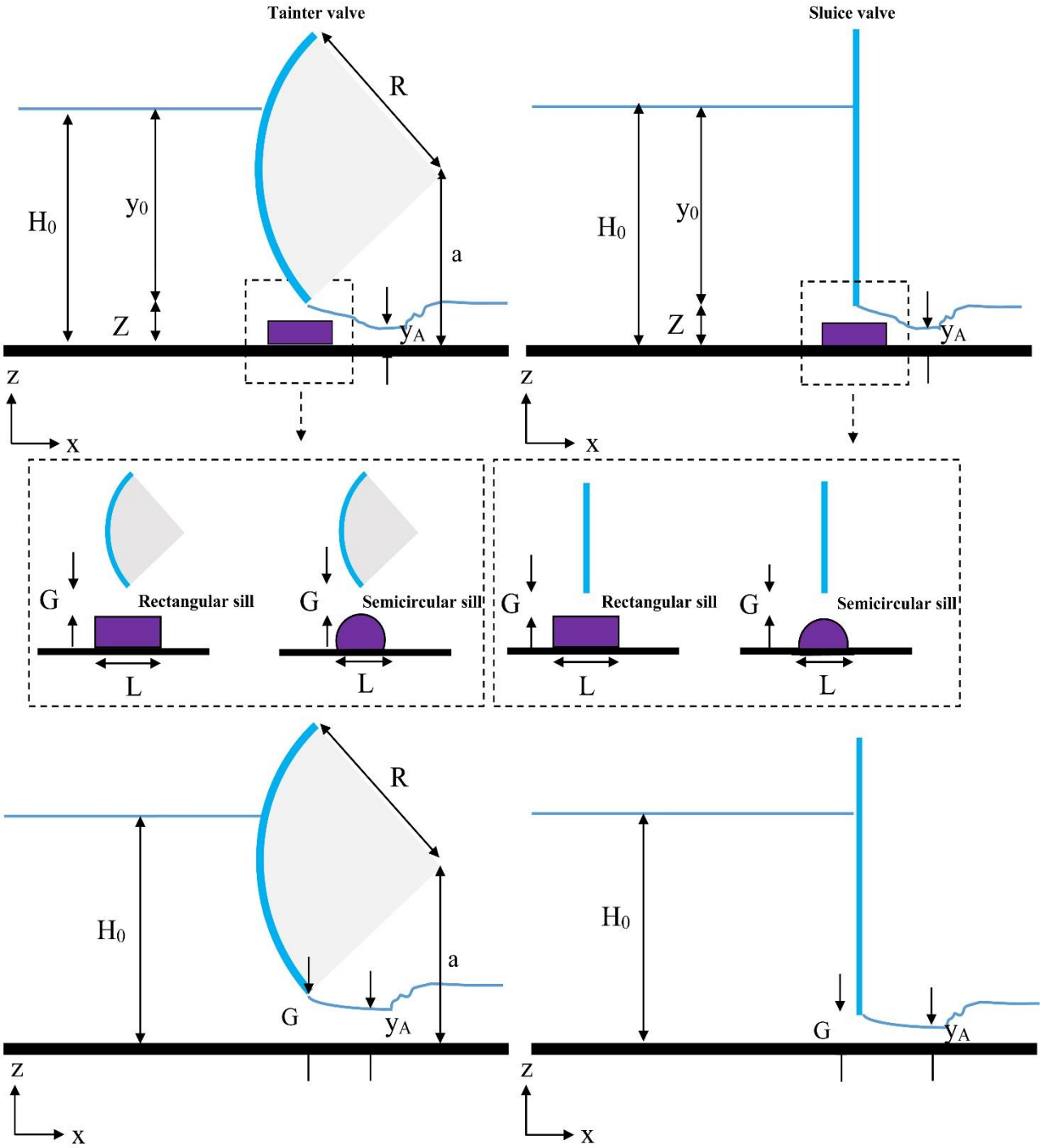

Fig. 1: Schematics of sluice and tainter gates with and without a sill (rectangular and semicircular)

The value of the normal sluice gate C_d is a function of relation (3) [5]:

$$C_d = \frac{q}{G\sqrt{2gH_0}} = f_1\left(\frac{H_0}{G}\right) \quad (3)$$

Here, C_d represents the discharge coefficient, H_0 represents the upstream depth, G represents the gate opening, q represents the discharge per unit width of the channel, and g represents the gravitational acceleration.

For a tainter gate, C_d is a function of the geometric parameters of the tainter gate such as R (the gate radius), and a (the height of the gate axis from the channel bottom). Using the π-Buckingham method, the key parameter affecting the tainter gate C_d are provided in Equation 4.

$$C_d = f_1\left(\frac{H_0}{G}\ \frac{R}{G}\ \frac{a}{G}\right) \quad (4)$$

For the case with a sill, the most significant parameters affecting C_d are:

$$f_1 = (C_d\ H_0\ G\ B\ Z\ L\ W\ \rho\ g\ \mu\ \sigma) = 0 \quad (5)$$

where B is the sill width, Z is the sill height, W is the channel width, σ is the surface tension, and L is the sill thickness.

Based on Buckingham's theory, the following relation can be presented:

$$f_2\left(C_d \ \frac{A_{total}}{B^2} \ \frac{H_0}{B} \ \frac{Z}{B} \ \frac{L}{B} \ \frac{W}{B} \ Re \ We\right) = 0 \quad (6)$$

Re (Reynolds number) and *We* (Weber number) parameters are co-dependent; they vary with the opening, so one of the two can be eliminated [20,23]. The flow is turbulent; therefore, the effect of Reynolds number can be neglected [24]. The final parameters are presented in Equation 7 [20]:

$$C_d = \frac{Q}{\left((A_1\sqrt{2gH_0})+(A_2\sqrt{2g(H_0-Z)})+(A_3\sqrt{2gH_0})\right)} = f_3\left(\frac{A_{total}}{B^2} \ \frac{H_0}{B} \ \frac{Z}{B} \ \frac{L}{B}\right) \quad (7)$$

Here, Q is the discharge and A_1, A_3, and A_2 are the flow regions (Fig. 2). For the tainter gate with a sill, the dimensionless parameters a/B and R/B are also shown in Equation 7.

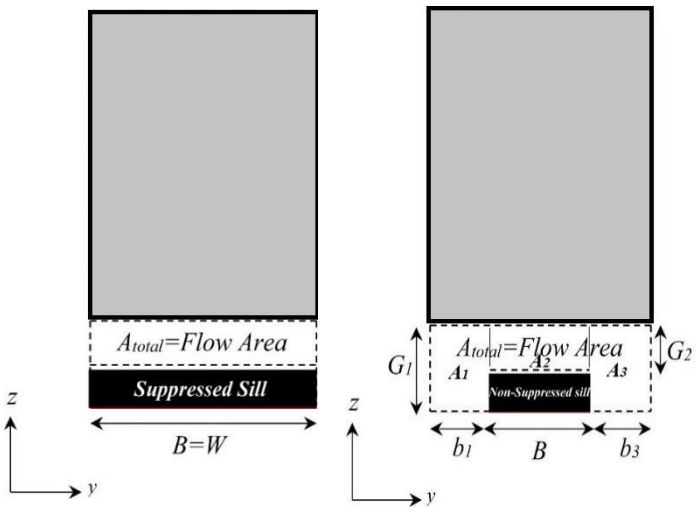

Fig. 2: Front view (y-z) of the gate-sill

2.3 Definition of solution network, boundary conditions and turbulence model

The 3D model and mesh network are depicted in Fig. 3. Here, two nested mesh blocks were utilized to conduct simulations. Table 2 displays the boundary conditions that were utilized.

The simulations were conducted with various mesh dimensions to obtain the optimal mesh. The comparison results are given in Table 3. In this study, to choose the best turbulence model, simulations were conducted with Re-Normalization Group (RNG), K-epsilon (k-ε), K-omega (k-ω), and Large Eddy Simulation (LES) turbulence models. Among these, the RNG was selected to continue the simulations. Comparing the findings of the mentioned models indicates that the RNG has less error than other models (Table 3). This issue has been seen in various research such as [25,26].

The following statistical indicators were used to check the performance of the simulation [27-40]. Each of these parameters provides valuable insights into different aspects of the model's performance. By analyzing the models using multiple parameters, the study was able to generate a more robust and reliable assessment of their overall performance. RE, RMSE close to zero, and KGE close to 1 (very good) show high precision of the results. Here, Cal and Obs represent the calculated and observation, σ is the standard deviation of the values, R is the correlation coefficient, and n is the total number of data

Relative Error

$$RE\% = \left|\frac{C_{d\,Obs} - C_{d\,Cal}}{C_{d\,Obs}}\right| \times 100 \quad (8)$$

Root Mean Square Error

$$RMSE = \sqrt{\frac{\sum_{i=1}^{n}\left(C_{d\,Obs} - C_{d\,Cal}\right)_i^2}{n}} \quad (9)$$

Kling Gupta Efficiency

$$KGE = 1 - \sqrt{(R-1)^2 + \left(\frac{\overline{C_{d\,Cal}}}{\overline{C_{d\,Obs}}} - 1\right)^2 + \left(\frac{\sigma_{Cal}/\overline{C_{d\,Cal}}}{\sigma_{Obs}/\overline{C_{d\,Obs}}} - 1\right)^2}$$

$$R = \frac{\left[\sum_{i=1}^{n}\left(C_{d\,Obs\,i} - \overline{C_{d\,Obs}}\right) \times \left(C_{d\,Cal\,i} - \overline{C_{d\,Cal}}\right)\right]}{\sum_{i=1}^{n}\left(C_{d\,Obs\,i} - \overline{C_{d\,Obs}}\right)\sum_{i=1}^{n}\left(C_{d\,Cal\,i} - \overline{C_{d\,Cal}}\right)} \quad (10)$$

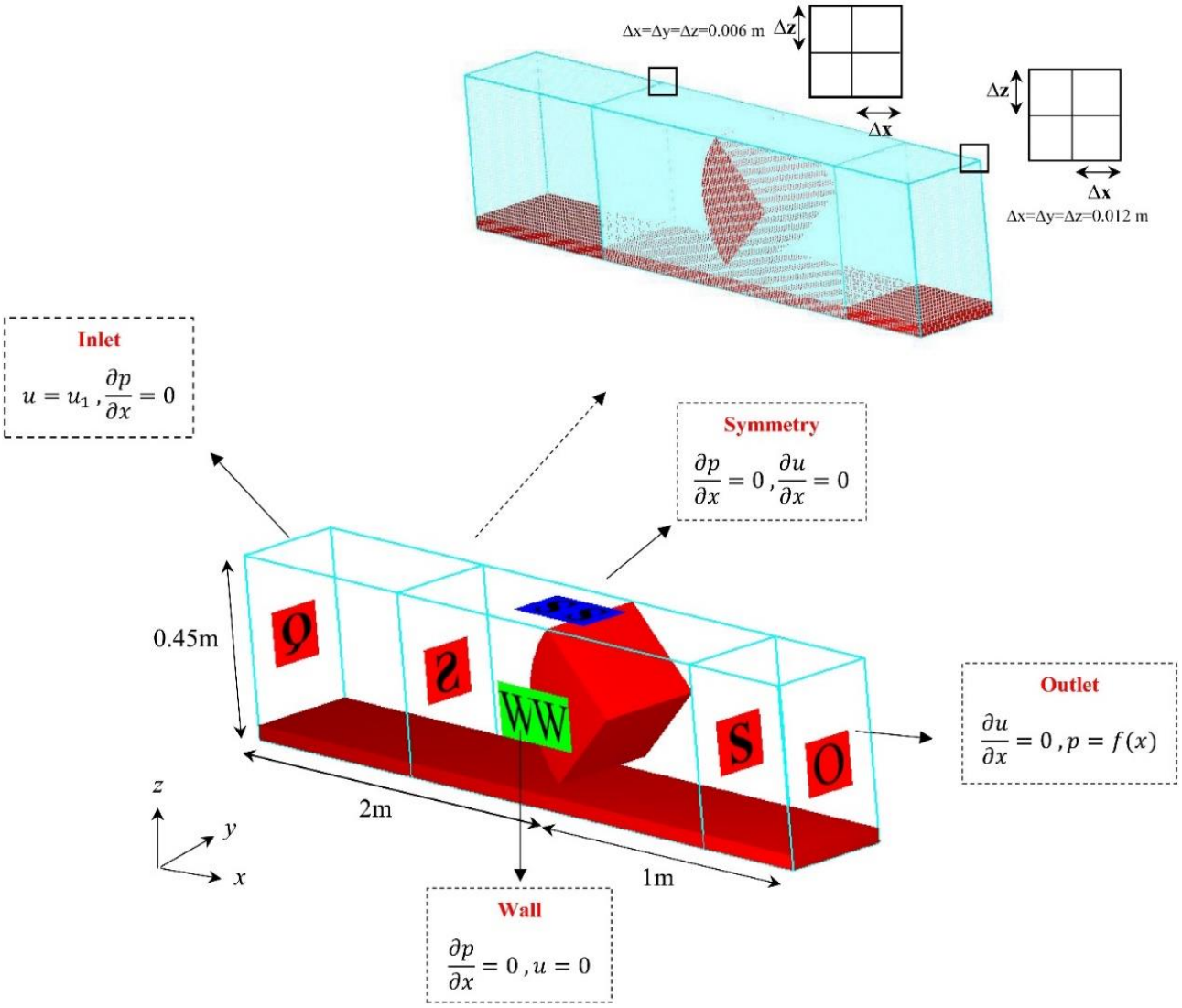

Fig. 3: Model with boundary conditions

Table 2: List of boundary condition

Mesh no.	Boundary condition			
	Inlet	Outlet	Top	Wall and Bottom
1st mesh block	Volume Flow Rate (VFR)	Output	Symmetry	Wall
2nd mesh block	Symmetry	Symmetry	Symmetry	Wall

3. Results and Discussion

The provided data in Table 3 facilitates a comparative analysis between numerical simulations and experimental observations, offering insights into the accuracy of the numerical models. Statistical indicators associated with varying mesh resolutions further contribute to the assessment of model performance. Upon examination of Table 3, mode 5 demonstrates favorable statistical results, suggesting a higher degree of congruence with experimental results. The similarity in statistical outcomes for modes 4 and 5 underscores the robustness of these mesh resolutions in capturing the underlying physics of the phenomena. In light of this similarity and the superior performance of mode 5, the decision to adopt mesh 4 continued simulations is based. This choice ensures a balance between computational efficiency and accuracy, streamlining the simulation process while upholding fidelity to experimental observations.

Table 3: Validation of the model

mode	Mesh block (m)	Mean RE (%)		RMSE		KGE		Turbulence models for mode 4	Model	RMSE	
		H_0	C_d	H_0 (m)	C_d (-)	H_0	C_d			H_0 (m)	C_d (-)
1	1st =0.014 2nd =0.007	14.12	9.28	0.0735	0.0914	good			RNG	0.0079	0.0117
2	1st =0.013 2nd =0.0065	6.35	5.72	0.0285	0.0348				k-ε	0.0085	0.0123
3	1st =0.012 2nd =0.007	3.90	2.95	0.0185	0.0245				k-ω	0.0094	0.0128
4	1st =0.012 2nd =0.006	2.94	1.60	0.0079	0.0117	very good			LES	0.0083	0.0120
5	1st =0.010 2nd =0.005	2.86	1.50	0.0076	0.0114						

Following the identification of the optimal mesh, the validation outcomes are delineated as shown in Fig. 4, encapsulating the models employed by Daneshfaraz et al. [20] across varying apertures of 0.01, 0.02, and 0.04 m. Harmony between numerical simulations and empirical observations is discernible. The Root Mean Square Error (RMSE) for the specified apertures are 0.0105, 0.0171, and 0.0148, respectively, reflecting concordance between the simulated and observed results. These low values of RMSE affirm the adequacy of the simulations.

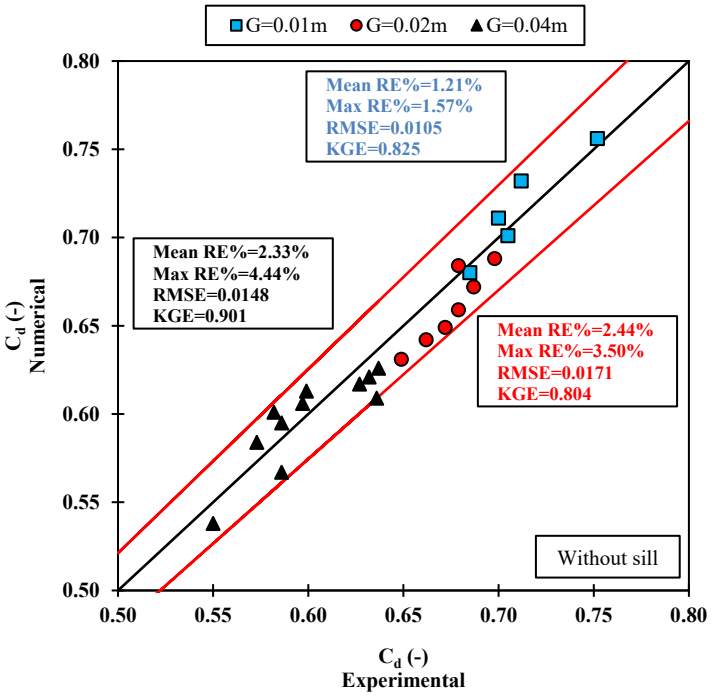

Fig. 4: Comparison of experimental and numerical results without a sill

In addition to validating the results without a sill and with openings of 0.01, 0.02, and 0.04 m that are presented in Fig. 4, a comparison of the numerical and experimental results was performed with sills of different widths of 0.15, 0.20, and 0.30 m. According to Fig. 5, it can be seen that the C_d obtained from the numerical solution differs slightly from the experimental data. In Fig. 5, statistical indicators are shown for each series of data. The results indicate good agreement. The mean RE%, maximum RE%, and RMSE for the suppressed sill are 1.50%, 1.76%, and 0.0118, respectively. In addition, the results for the non-suppressed 0.20 m sill are 1.98%, 2.65%, and 0.0143, respectively. For the non-suppressed 0.15 m sill the corresponding results are 1.16%, 2.21% and 0.0082, respectively.

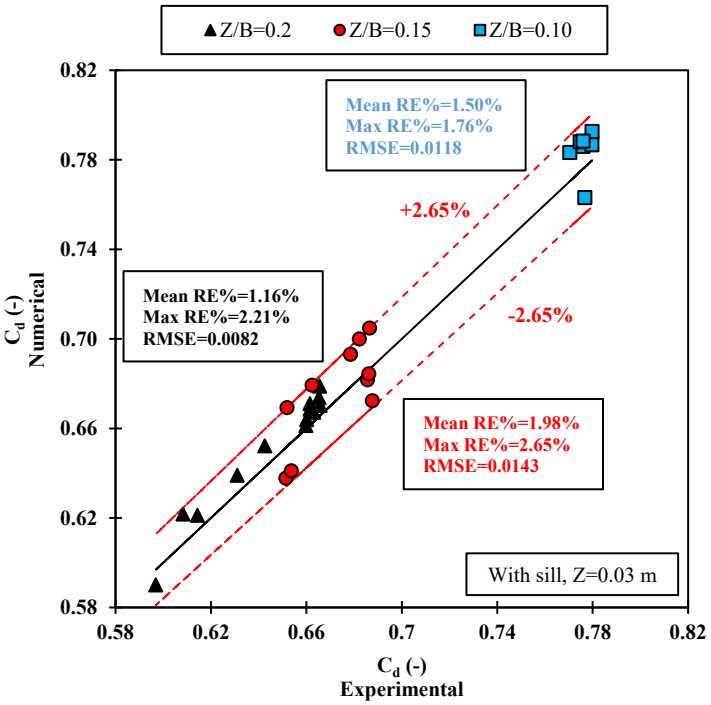

Fig. 5: The results in the case with suppressed, and non-suppressed sill

Subsequently, the outcomes of alternative models have undergone scrutiny. Illustrated in Fig. 6a is the C_d pertaining to both sluice and tainter gates. Notably, the C_d values associated with the tainter gate consistently surpass those of the sluice gate. This discrepancy, as delineated in Fig. 6b, can be attributed to the geometric configuration of the gates. Specifically, Fig. 6b elucidates the velocity profile along the x-z section within both sluice and tainter gates, thus unveiling the discernible influence of gate morphology on flow dynamics. This depiction underscores the pivotal role of gate design in modulating flow patterns within hydraulic systems.

In Fig. 7, the effects of rectangular and semicircular sills on the C_d of sluice and tainter gates with different openings are shown. According to Fig. 7, C_d increases with the increase of B. The increase of C_d with the increase in B can be attributed to the uniform distribution of the flow towards the gate. For sills with smaller widths, the opening area on the sides of the sill is greater than that above the sill. This increases the outflow from the sides compared to the top of the sill. Flow returns towards the gate and causes an increase in energy loss and turbulence of the output flow from the gate. This leads to a decrease in C_d (Fig. 8). In Fig. 8, the streamlines shown in section y-z are related to the non-suppressed sill. According to Fig. 7, the highest C_d corresponds to the semicircular sill. With a semicircular sill, the water passes over the sill smoothly and uniformly after impacting the sill. On the other hand, with a rectangular sill, some of the streamlines reverse after impacting the sill and an eddy is created there. The tainter gate has a larger C_d than does the sluice gate

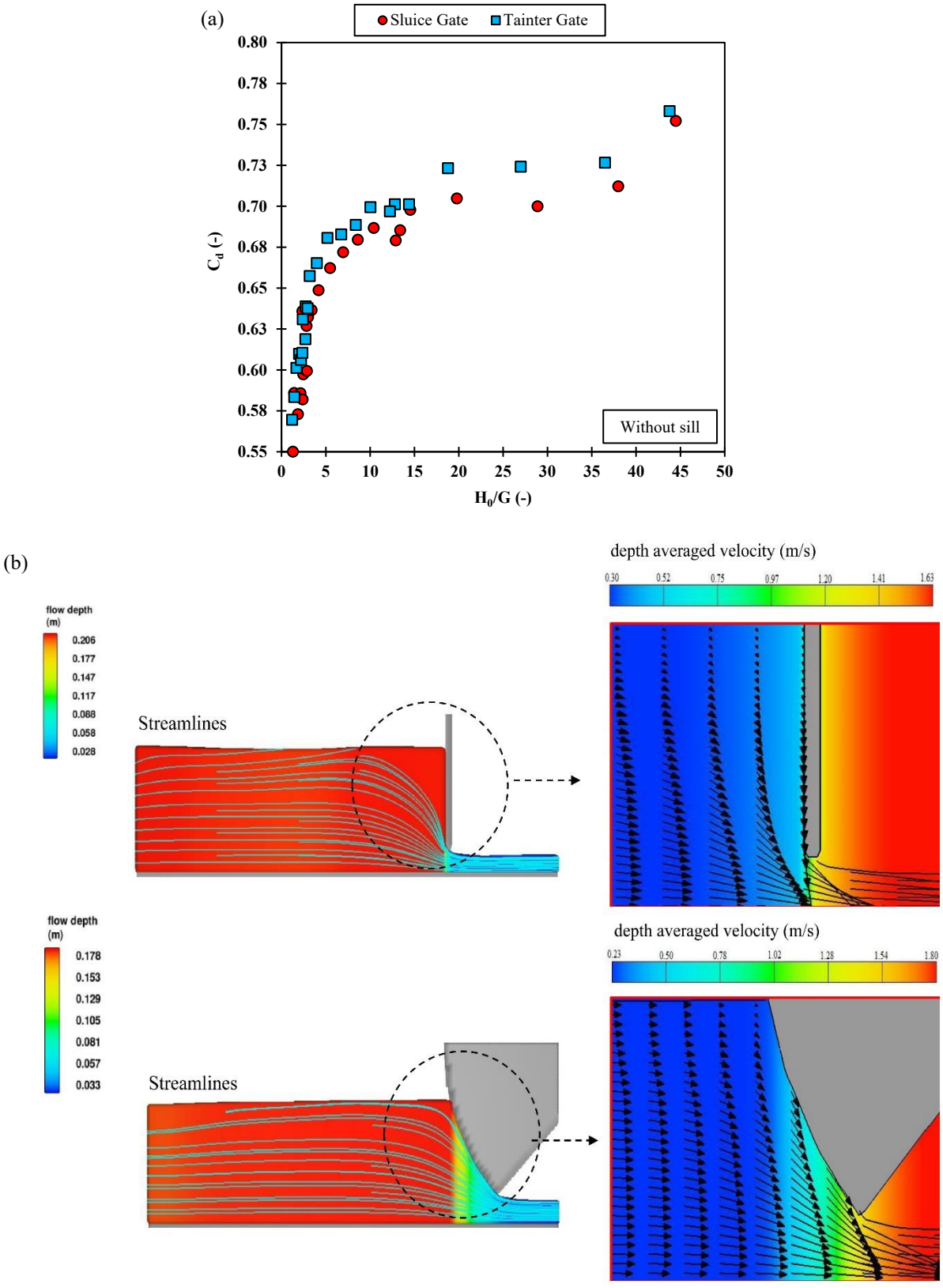

Fig. 6: a) C_d of sluice and tainter gates without a sill, b) flow patterns for sluice and tainter gates

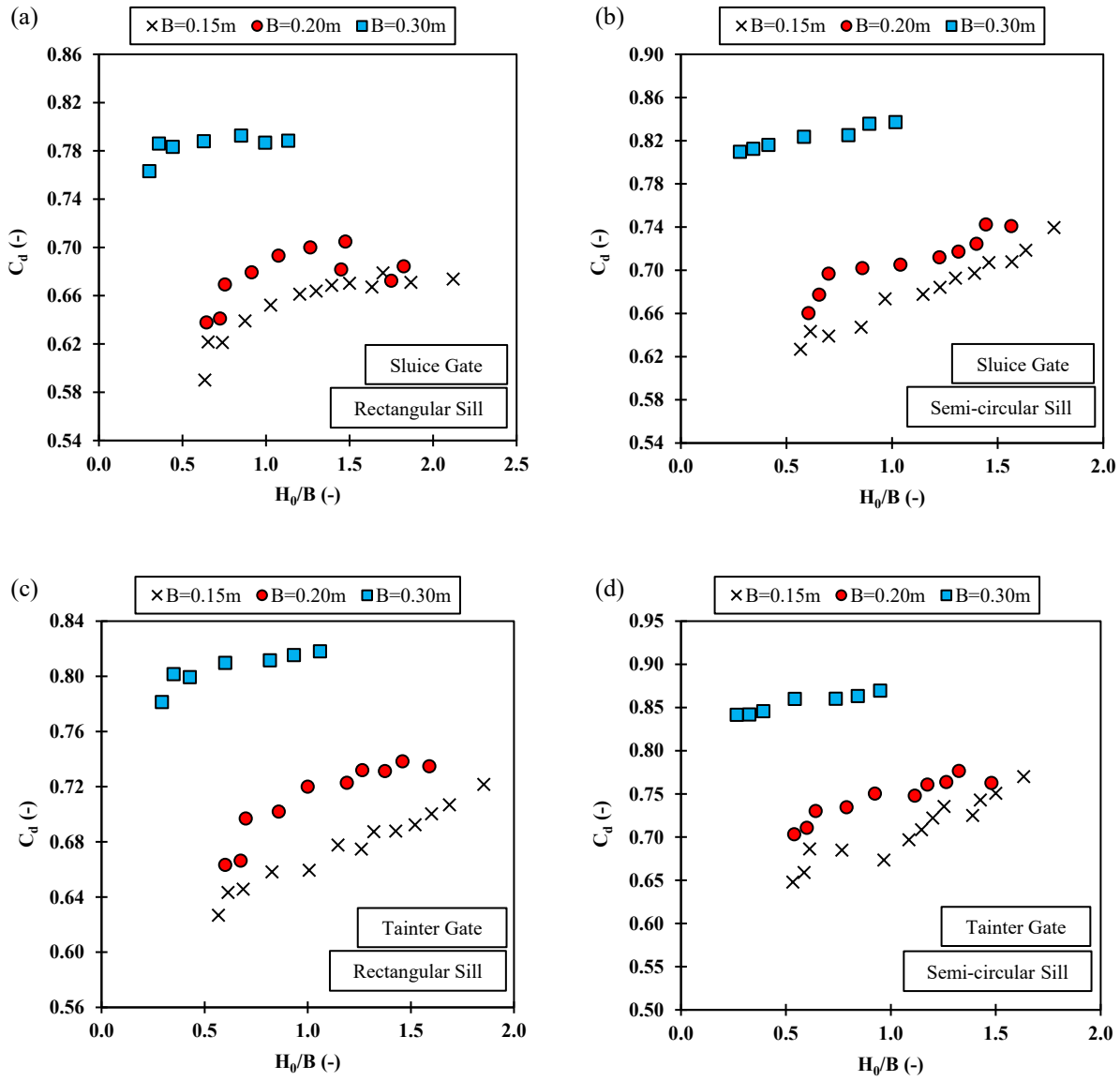

Fig. 7: C_d of sluice and tainter gates with various widths (rectangular and semicircular sills)

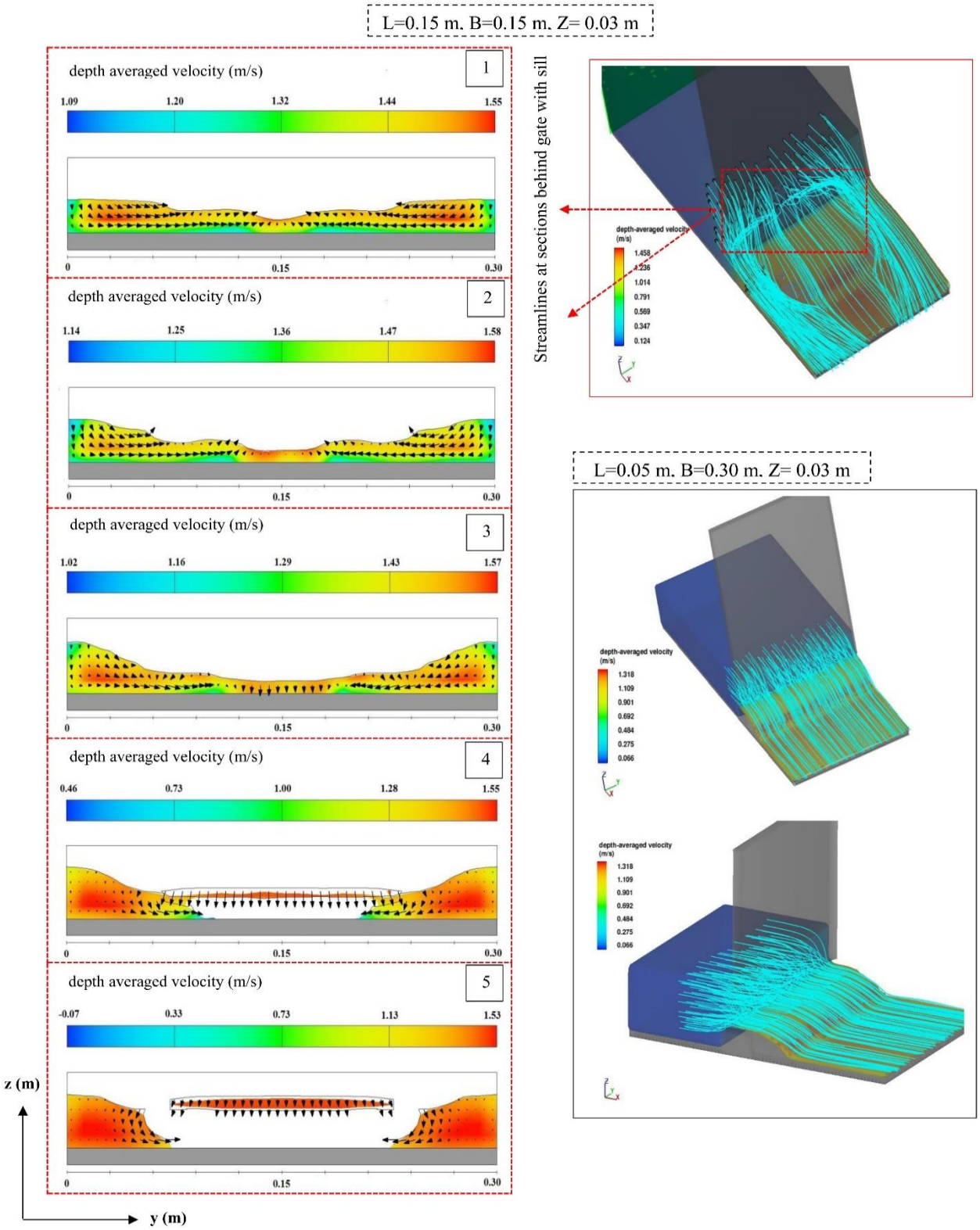

Fig. 8: Pattern and streamlines with a non-suppressed sill of 0.20 m and a suppressed sill of 0.30 m

It is evident that adding a sill, increases the C_d and improves the performance of the system (Fig. 9). The comparison between the C_d for various openings in the condition with a sill shows a decrease in C_d compared to the gate with a smaller gate opening. Since the shape of the gate and sill alters the trajectory of the streamlines, it significantly influences the C_d.

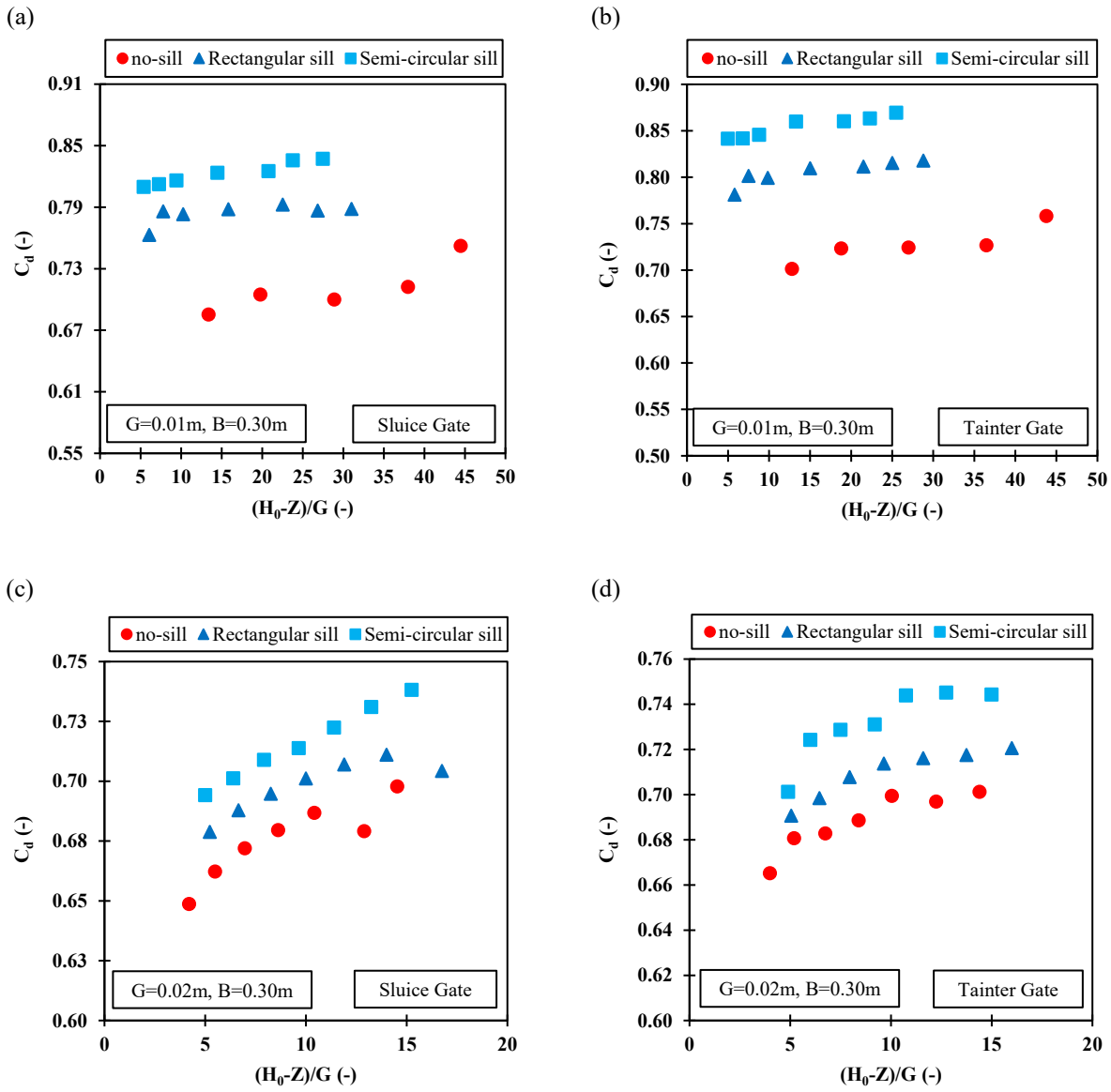

Fig. 9: C_d for sluice and tainter gates without and with a sill

The sill with heights of 0.03, 0.06, and 0.09 m were considered for rectangular and semicircular sills. As can be seen, the C_d in all cases is higher than without a sill (Fig. 10). In addition, C_d with a rectangular sill increases for Z/B up to 0.20 but decreases for Z/B of 0.30 compared to a sill with Z/B=0.20. In Fig. 10b, with the increase of Z/B up to 0.10, the C_d increases, and then later decreases. The C_d of semicircular sills with Z/B of 0.20 and 0.30 have similar results. Increasing Z leads to an increase in the upstream depth and pressure increases. However, using a sill leads to a reduction in the depth above the sill and in pressure near the gate opening. Reducing the pressure there causes suction and decreases the water depth compared to the situation without a sill, in which the C_d increases.

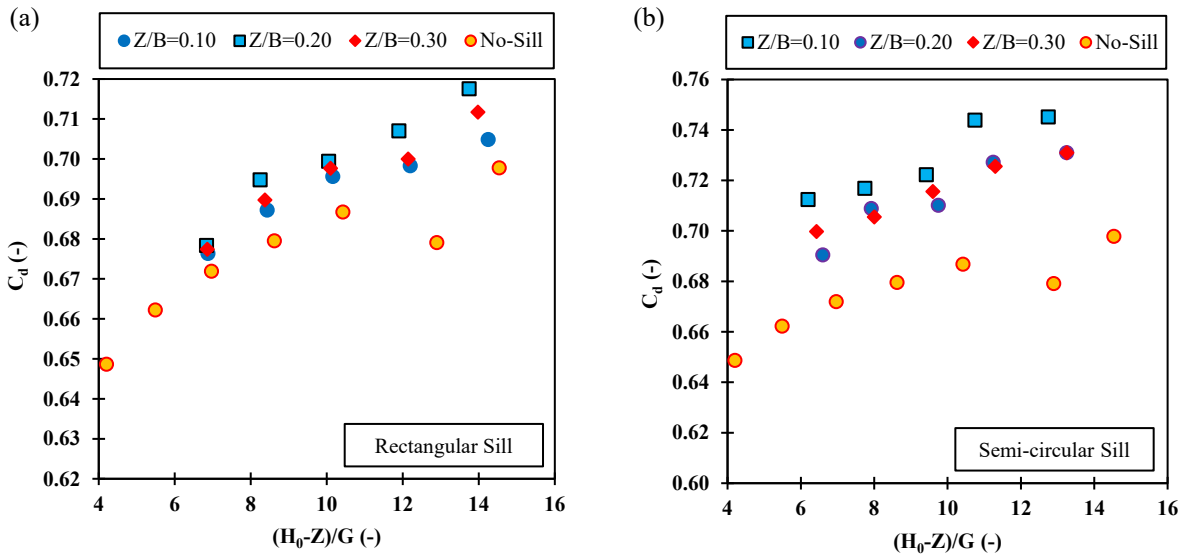

Fig. 10: The sill height effect on the C_d a) Rectangular sill b) Semicircular sill

According to Fig. 11a, increasing L increases friction with a sill, which has a direct relationship with the flow shear stress (τ). As the gate gets closer, τ behind it increases (rectangular sill). For the rectangular sill at the beginning of the sill, τ increases due to the proximity to the sill wall. In addition, a sudden increase is observed at the end of the sill. In the downward position, τ increases and decreases along the sill. τ in the semicircular sill is lower compared to the rectangular sill, which leads to a reduction in friction and a decrease in the upstream flow depth. By increasing L, τ on both the surface and sides of the sill increases. The boundary layer on the sides of the non-suppressed sill is also subject to shear stress, which diminishes as distance increases. This matter also affects C_d. The thickening leads to a reduction of C_d. (Figs. 11b and 11c). With suppressed sills, due to the absence of a boundary layer between the sill and the non-sill part, there is no shear stress in that part, and τ is caused by the thickness of the sill and walls.

Here, nonlinear polynomial regression equations were presented to estimate C_d. Equations 11 and 12 are presented for sluice and tainter gates. In Figs. 12a and 12b, the accuracy of Equations (11) and (12) are shown.

$$C_d = -1{,}254\left(\frac{A_{total}}{B^2}\right)^{0{,}225} + 0{,}089\left(\frac{H_0}{B}\right)^{0{,}536} + 1{,}212\left(\frac{Z}{B}\right)^{-0{,}005} + 2{,}445\left(\frac{L}{B}\right)^{1{,}833} \quad (11)$$

$$C_d = -9.54\left(\frac{A_{total}}{B^2}\right)^{0.021} - 7.003\left(\frac{H_0}{B}\right)^{-0.008} - 0.636\left(\frac{Z}{B}\right)^{3.952} + 10.598\left(\frac{L}{B}\right)^{0.022} + 1.033\left(\frac{R}{B}\right)^{0.246} + 5.536\left(\frac{a}{B}\right)^{-0.023}. \quad (12)$$

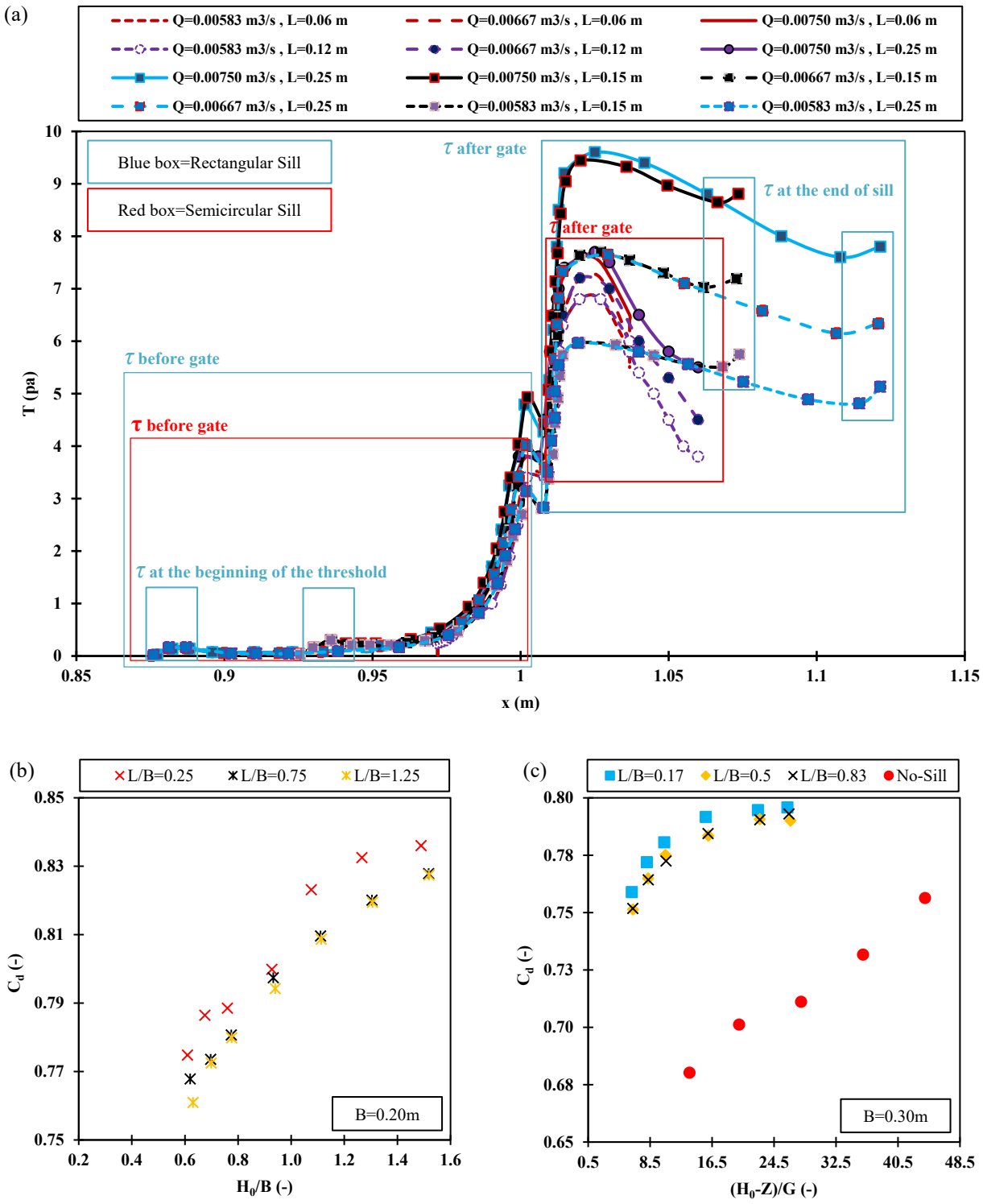

Fig. 11: a) Diagram of shear stress b, c) C_d values with various sill thicknesses

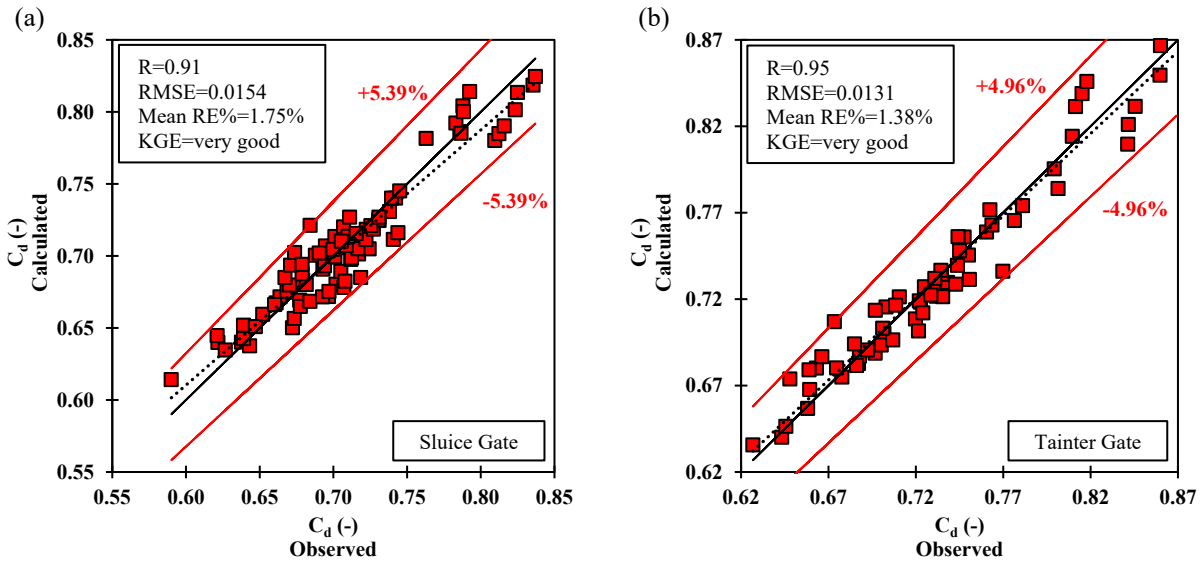

Fig. 12: Comparison values of the C_d with a sill a) sluice gate, b) tainter gate

4. Conclusions

In this study, numerical investigations were conducted to analyze the flow characteristics within sluice and tainter gates. Simulations were executed across a spectrum of discharge rates, ranging from 0.0025 to 0.0142 m^3/s and upstream depths, spanning from 0.05 to 0.44 m. Notably, the RNG turbulence model demonstrated superior accuracy compared to alternative models such as k-ε, k-ω, and LES turbulence models. Analysis of the results unveiled that the tainter gate exhibited the highest C_d among the investigated configurations. Furthermore, comparative assessment between C_d values with and without a sill underscored the enhanced performance associated with the presence of a sill, indicative of augmented C_d. Intriguingly, the semicircular sill displayed a superior C_d relative to the rectangular sill, attributed chiefly to its distinctive geometric profile. Moreover, juxtaposing C_d values with and without a suppressed sill for similar gate openings revealed a discernible reduction in upstream flow depth in the presence of a sill. This phenomenon engendered a corresponding decrease in pressure exerted on the gate, thereby resulting in an amplified C_d. Notably, across all sill heights, C_d consistently exceeded values obtained in scenarios devoid of a sill. Additionally, a constant ratio of (y_0/G) exhibited an incremental trend with increasing sill height, subsequently reaching a threshold beyond which a decline was observed. Furthermore, augmenting sill thickness precipitated an escalation in shear stress across all non-suppressed and suppressed sill configurations, consequently eliciting a decrease in C_d with increasing sill thickness. These findings illuminate the intricate interplay between gate design, sill morphology, and flow dynamics, thereby elucidating pivotal insights for hydraulic system optimization and design refinement.

Acknowledgements

The authors of this article would like to thanks all those who accompanied us in writing this article.

References

[1] Negm, A. M., Alhamid, A. A., & El-Saiad, A. A. (1998). Submerged flow below sluice gate with s sill. Proceedings of International Conference on Hydro-Science and Engineering Hydro-Science and Engineering ICHE98, Advances in Hydro-Science and Engineering, Vol.III, Published on CD-Rom and A Booklet of Abstracts, 31 Aug.-3 Sep 1998. Cottbus/Berlin.

[2] Henry, H. R. (1950). Discussion on "Diffusion of submerged jets, "by Albertson, M. L. et al., Trans. Am. Society Civil Engrs. 115:687.

[3] Rajaratnam, N., & Subramanya, K. (1967). Flow equation for the sluice gate. Journal of the Irrigation and Drainage Division, 93(3), 167-186.

[4] Rajaratnam, N. (1977). Free flow immediately below sluice gates. Journal of the Hydraulics Division, 103(4), 345-351.

[5] Swamee, P. K. (1992). Sluice-gate discharge equations. Journal of Irrigation and Drainage Engineering, 118(1), 56-60.

[6] Shivapur, A. V., & Shesha Prakash, M. N. (2005). Inclined sluice gate for flow measurement. ISH Journal of Hydraulic Engineering, 11(1), 46-56.

[7] Bijankhan, M., Kouchakzadeh, S., & Bayat, E. (2011). Distinguishing condition curve for radial gates. Flow Measurement and Instrumentation, 22(6), 500-506.

[8] Daneshfaraz, R., Ghahramanzadeh, A., Ghaderi, A., Joudi, A. R., & Abraham, J. (2016). Investigation of the effect of edge shape on characteristics of flow under vertical gates. Journal-American Water Works Association, 108(8), E425-E432.

[9] Shayan, H. K., Farhoudi, J., & Vatankhah, A. (2021). Experimental and field verifications of radial gates as flow measurement structures. Water Supply, 21(6), 3057-3079.

[10] Salmasi, F., Nouri, M., Sihag, P., & Abraham, J. (2021). Application of SVM, ANN, GRNN, RF, GP and RT models for predicting discharge coefficients of oblique sluice gates using experimental data. Water Supply, 21(1), 232-248.

[11] Roushangar, K., Alirezazadeh Sadaghiani, A., & Shahnazi, S. (2023). Novel application of robust GWO-KELM model in predicting discharge coefficient of radial gates: a field data-based analysis. Journal of Hydroinformatics, 25(2), 275-299.

[12] Alhamid, A. A. (1999). Coefficient of discharge for free flow sluice gates. Journal of King Saud University-Engineering Sciences, 11(1), 33-47.

[13] Abdelhaleem, F. S. F. (2017). Hydraulics of submerged radial gates with a sill. ISH Journal of Hydraulic Engineering, 23(2), 177-186.

[14] Salmasi. F., & Norouzi Sarkarabad, R. (2018). Investigation of different geometric shapes of sills on discharge coefficient of vertical sluice gate. Amirkabir Journal of Civil Engineering 52(1), 26-31.

[15] Salmasi, F., Nouri, M., & Abraham, J. (2019). Laboratory study of the effect of sills on radial gate discharge coefficient. KSCE Journal of Civil Engineering, 23(5), 2117-2125.

[16] Karami, S., Heidari, M. M., & Rad, M. H. A. (2020). Investigation of free flow under the sluice gate with the sill using flow-3D model. Iranian Journal of Science and Technology, Transactions of Civil Engineering, 44(1), 317-324.

[17] Ghorbani, M. A., Salmasi, F., Saggi, M. K., Bhatia, A. S., Kahya, E., & Norouzi, R. (2020). Deep learning under H2O framework: A novel approach for quantitative analysis of discharge coefficient in sluice gates. Journal of Hydroinformatics, 22(6), 1603-1619.

[18] Norouzi, R., Ebadzadeh, P., Sume, V., & Daneshfaraz, R. (2023). Upstream vortices of a sluice gate: An experimental and numerical study. AQUA—Water Infrastructure, Ecosystems and Society, 72(10), 1906-1919.

[19] Hassanzadeh, Y., & Abbaszadeh, H. (2023). Investigating discharge coefficient of slide gate-sill combination using expert soft computing models. Journal of Hydraulic Structures, 9(1), 63-80.

[20] Daneshfaraz, R., Norouzi, R., Abbaszadeh, H., & Azamathulla, H. M. (2022). Theoretical and experimental analysis of applicability of sill with different widths on the gate discharge coefficients. Water Supply, 22(10), 7767-7781.

[21] Daneshfaraz, R., Norouzi, R., Abbaszadeh, H., Kuriqi, A., & Di Francesco, S. (2022). Influence of sill on the hydraulic regime in sluice gates: an experimental and numerical analysis. Fluids, 7(7), 244.

[22] Flow Science Inc. (2016) FLOW-3D V 11.2 User's Manual, Santa Fe, NM, USA.

[23] Lauria, A., Calomino, F., Alfonsi, G., & D'Ippolito, A. (2020). Discharge coefficients for sluice gates set in weirs at different upstream wall inclinations. Water, 12(1), 245.

[24] Nasrabadi, M., Mehri, Y., Ghassemi, A., & Omid, M. H. (2021). Predicting submerged hydraulic jump characteristics using machine learning methods. Water Supply, 21(8), 4180-4194.

[25] Cassan, L., & Belaud, G. (2012). Experimental and numerical investigation of flow under sluice gates. Journal of Hydraulic Engineering, 138(4), 367-373.

[26] Valero, D., Bung, D. B., Erpicum, S., Peltier, Y., & Dewals, B. (2022). Unsteady shallow meandering flows in rectangular reservoirs: A modal analysis of URANS modelling. Journal of Hydro-environment Research, 42, 12-20.

[27] Gupta HV, Kling H, Yilmaz KK, Martinez GF (2009) Decomposition of the mean squared error and NSE performance criteria: Implications for improving hydrological modelling. J. Hydrol. 377:80–91. https://doi.org/10.1016/j.jhydrol.2009.08.003.

[28] Abbaszadeh, H., Daneshfaraz, R., Sume, V., & Abraham, J. (2024). Experimental investigation and application of soft computing models for predicting flow energy loss in arc-shaped constrictions. AQUA—Water Infrastructure, Ecosystems and Society, 73(3), 637-661.

[29] Hassanzadeh, Y., Abbaszadeh, H., Abedi, A., & Abraham, J. (2024). Numerical simulation of the effect of downstream material on scouring-sediment profile of combined spillway-gate. AQUA—Water Infrastructure, Ecosystems and Society, 73(12), 2322-2343.

[30] Abbaszadeh, H., Norouzi, R., Sume, V., Kuriqi, A., Daneshfaraz, R., & Abraham, J. (2023). Sill role effect on the flow characteristics (experimental and regression model analytical). Fluids, 8(8), 235.

[31] Daneshfaraz, R., Norouzi, R., & Abbaszadeh, H. (2021). Numerical investigation on effective parameters on hydraulic flows in chimney proportional weirs. Iranian Journal of Soil and Water Research, 52(6), 1599-1616.

[32] Roushangar, K., Goodarzi, S., & Abbaszadeh, H. (2024). Numerical investigation of the performance of blade groynes on scouring and its effect on hydraulic parameters of sediment and flow. Environment and Water Engineering, 10(1), 121-136.

[33] Ebadzadeh, P., Abbaszadeh, H., Daneshfaraz, R., & Abraham, J. (2025). Enhancing energy dissipation in stepped weirs: numerical analysis and machine learning of ANN, SVM and non-linear regression predictions. Multiscale and Multidisciplinary Modeling, Experiments and Design, 8(8), 345.

[34] Abbaszadeh, H., & Tarinejad, R. (2025). Soft Computing and Predicting Labyrinth Gates Discharge Coefficient. Water Resources, 52(4), 701-714.

[35] Azamathulla, H. M., Haghiabi, A. H., & Parsaie, A. (2016). Prediction of side weir discharge coefficient by support vector machine technique. Water Science and Technology: Water Supply, 16(4), 1002-1016.

[36] Abbaszadeh, H., Norouzi, R., Süme, V., Daneshfaraz, R., & Tarinejad, R. (2023). Discharge coefficient of combined

rectangular-triangular weirs using soft computing models. Journal of Hydraulic Structures, 9(1), 98-110.

[37] Haghiabi, A. H., Parsaie, A., & Ememgholizadeh, S. (2018). Prediction of discharge coefficient of triangular labyrinth weirs using Adaptive Neuro Fuzzy Inference System. Alexandria Engineering Journal, 57(3), 1773-1782.

[38] Daneshfaraz, R., Sadeghfam, S., Adami, R., & Abbaszadeh, H. (2023). Numerical analysis of seepage in steady and transient flow state by the radial basis function method. Numerical Methods in Civil Engineering, 8(1), 58-68.

[39] Abbaszadeh, H., Ebadzadeh, P., Daneshfaraz, R., & Norouzi, R. (2024). Investigating and predicting hydraulic jump energy loss with threshold (Experimental and regression analysis). Journal of Hydraulic Structures, 10(2), 46-54.

[40] Daneshfaraz, R., Norouzi, R., Ebadzadeh, P., & Abbaszadeh, H. (2022). Numerical investigation on effective parameters on hydraulic flows in a sluice gate with sill on free-flow condition. Environment and Water Engineering, 8(3), 711-725.